Korean J. Chem. Eng., **31**(3), 503-508 (2014)
DOI: 10.1007/s11814-013-0233-2

pISSN: 0256-1115
eISSN: 1975-7220

Fabrication and characterization of NiO nanoparticles by precipitation from aqueous solution

Javad Moghaddam† and Elham Hashemi

Materials and Metallurgical Engineering Department, Advanced Materials Research Center, Sahand University of Technology, Tabriz, Iran
(*Received 10 July 2013 • accepted 3 November 2013*)

Abstract−Present work involves synthesis of NiO nanoparticles using chemical homogeneous precipitation (CHP) method as a facile procedure. Ammonia as a complex agent was used in this method. Effects of different types of complexation-precipitation methods on the crystallinity and morphology of nanoparticles were investigated. NiO particles were prepared by direct precipitation method from $NiSO_4$ solution to compare crystallinity and morphology of NiO particles with particles obtained via complexation-precipitation methods. Our major intent was to investigate the effect of complex agent on the crystallization and growth of NiO nanoparticles. Results showed that the best condition for synthesizing spherical NiO shape was using NaOH as decomposing agent, of which the consequence was more uniformity and spherical nanoparticles with a diameter in the range of 40-60 nm. The size of the nickel oxide and nickel hydroxide nanoparticles was estimated by X-ray powder diffraction (XRD) pattern. The chemical structure information of the particles was studied by Fourier transform infrared (FT-IR) spectroscopy. Spherical, elliptical, sheet or flower-like shapes were detected by field emission scanning electron microscopy (FESEM) analysis. Results showed that by the use of ammonia as complex agent, crystalline state and particles size distribution of NiO nanoparticles improved.

Keywords: Complex Precipitation, Nickel Oxide, Nanoparticles, Nickel Hydroxide, Chemical Homogeneous Precipitation (CHP)

INTRODUCTION

Nanostructured materials with functional properties have attracted much attention in recent years due to their unique physical and chemical properties based on the size-quantization effect and large specic surface area. Crystallography, morphology and size of the nanomaterials will greatly affect their optical, electronic, magnetic and chemical properties [1-3]. Therefore, synthesizing nanomaterials with controlled morphology becomes a major challenge. Nickel oxide (NiO), a p-type semiconductor [4], is widely used, such as in gas sensors [5], electrochromic lms [6], catalysis [7], fuel cell electrodes [8], and magnetic materials [9]. Because of its great physical and chemical properties [10-13], nanoscale nickel oxide has attracted tremendous interest, and various novel nickel oxide nanostructures have been fabricated, e.g., nanoparticles [14], nanosheets [15], nanorods [16], nanowires [17], hollow spheres [18] and porous solids [19]. Three-dimensionally ordered architectures assembled by the low-dimensional building blocks are also reported recently [20-25]. However, the search for developing a facile and feasible method to synthesize hierarchical structures is still a challenging process.

In recent years, scientists have synthesized nano-NiO materials with controlled morphology because of the high dependency of NiO characterization on their size and shape. Different methods like complexation-precipitation [2], hydrothermal [26], sol-gel [27], thermal decomposition [28] and mechano-chemical route [29] are used to synthesize NiO nanopowders. However, most of the reported experimental techniques for the synthesis of nanopowders are still limited in laboratory scale due to some insurmountable problems and also intricate circumstances such as special conditions, tedious procedures, complex apparatus, low-yield and high-cost. It is essential to develop a way to manufacture high-quality nanopowders at high throughput with low cost. Among the above-mentioned methods, complexation-precipitation is a simple way to fabricate NiO nanopowders. Various parameters like pH, temperature and precipitation mechanism can play a significant effect on the morphology of NiO powders [30-34].

We tried to obtain different conditions for synthesis of NiO nanopowders by complexation-precipitation method using $NiSO_4.6H_2O$ as the raw material. Consequently, nickel oxide nano particles were successfully prepared by controlling the effective parameters. In addition, different precipitation methods such as precipitation with NaOH, diluting and heating of solution were used to decompose the Ni^{2+} complex. The effects of various complexation-precipitation methods have been studied by comparing complex precipitation with direct precipitation methods.

EXPERIMENTAL PROCEDURE

1. Materials

Chemicals such as nickel sulfate hexahydrate ($NiSO_4{\cdot}6H_2O$, 99.95% Merck), sodium hydroxide (NaOH, 99.95% Merck), ammonia (NH_3, 25%) were of analytical grade and used without further purification. Deionized water was used throughout the study.

2. Methods

In a typical experiment, 2.63 g $NiSO_4{\cdot}6H_2O$ was dissolved in 100 mL distilled water under magnetic stirring to form a homoge-

†To whom correspondence should be addressed.
E-mail: moghaddam@sut.ac.ir, hastyir@yahoo.com

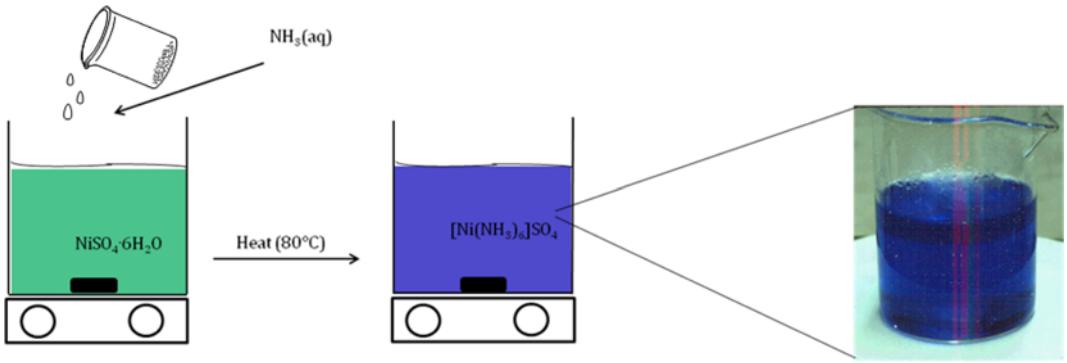

Fig. 1. Schematic for produce of ammonia complex.

neous solution at room temperature (0.1 M solution of $NiSO_4 \cdot 6H_2O$). This solution was heated to 80 °C. Then, ammonia solution was added to $NiSO_4 \cdot 6H_2O$ solution for achieving pH=11 (Ammonia Complex, Eq. (1)).

$$NiSO_4 \cdot 6H_2O + 6NH_3 \rightarrow Ni(NH_3)_6SO_4 + 6H_2O \quad (1)$$

This solution was kept at 80 °C until it turned dark blue, which indicates the formation of $[Ni(NH_3)_6]^{2+}$ complex. The Schematic of above-mentioned procedure has been presented in Fig. 1.

Afterward, decomposition of $[Ni(NH_3)_6]^{2+}$ complex operations were conducted through the following three different methods:

(a) 0.2 M sodium hydroxide solution was slowly added to the solution to form $Ni(OH)_2$ precipitates. This process continued until the solution became completely colorless (Eq. (2)).

$$[Ni(NH_3)_6]SO_4 + 2NaOH \rightarrow Ni(OH)_2 + Na_2SO_4 + 6NH_3 \quad (2)$$

(b) The second approach involved heating the solution at 90 °C, until ammonia content of solution was evaporated (Eq. (3) and (4)).

$$[Ni(NH_3)_6]SO_4 + 2H_2O \xrightarrow{Heat} Ni(OH)_2 + (NH_4)SO_4 + 4NH_3\uparrow \quad (3)$$

$$[Ni(NH_3)_6]SO_4 + H_2O \xrightarrow{Heat} Ni(OH)_x + (SO_4)_y + 6NH_3\uparrow \quad (4)$$

(c) The final method was diluting the $[Ni(NH_3)_6]^{2+}$ complex solution [35]. Deionized water was dropwise added to the solution (Eq. (5)).

$$[Ni(NH_3)_6]SO_4 \xrightarrow{Diluting\ by\ H_2O} Ni(OH)_x + (SO_4)_y + 6NH_3 \quad (5)$$

A schematic diagram of the above-mentioned method procedures is presented in Fig. 2.

In addition, as demonstrated in Fig. 3, NiO particles were prepared by direct precipitation method from $NiSO_4$ solution to compare crystallinity and morphology of NiO particles with particles obtained via complexation-precipitation methods. The amount of 0.5 M NaOH was slowly added to 0.5 M $NiSO_4$ solution. This pro-

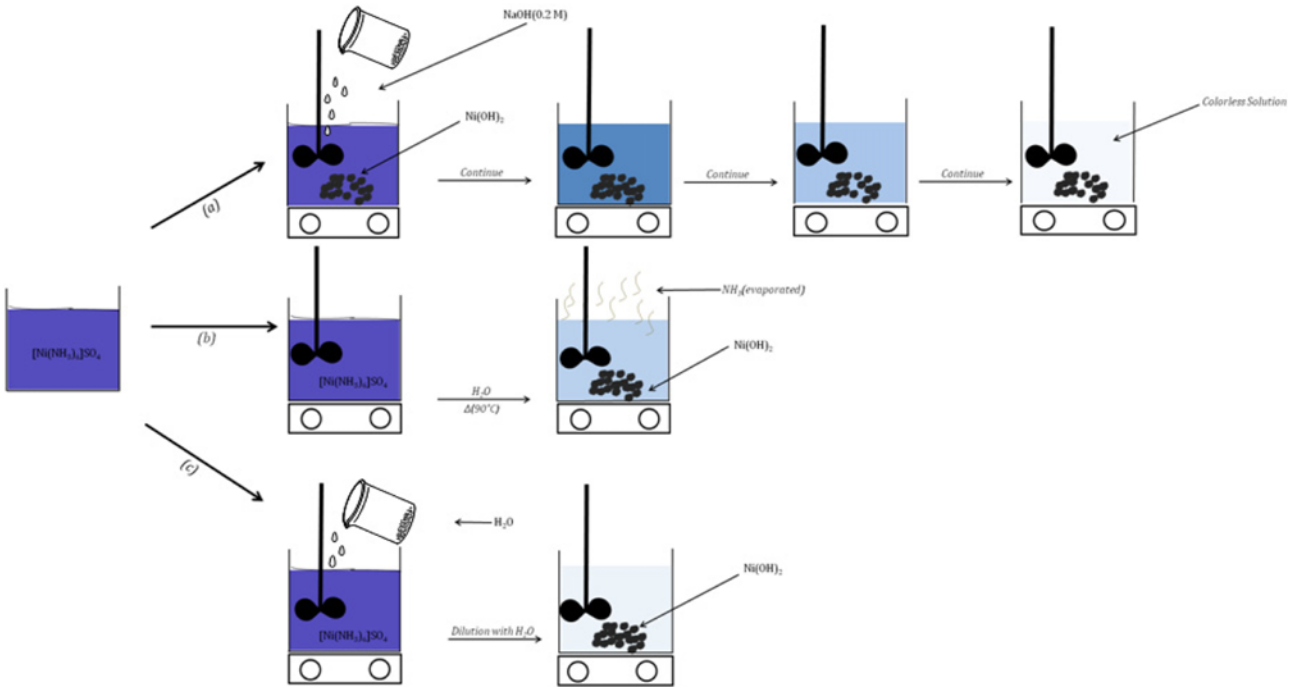

Fig. 2. Schematic diagrams of three precipitation methods by; (a) NaOH (b) heating and (c) diluting.

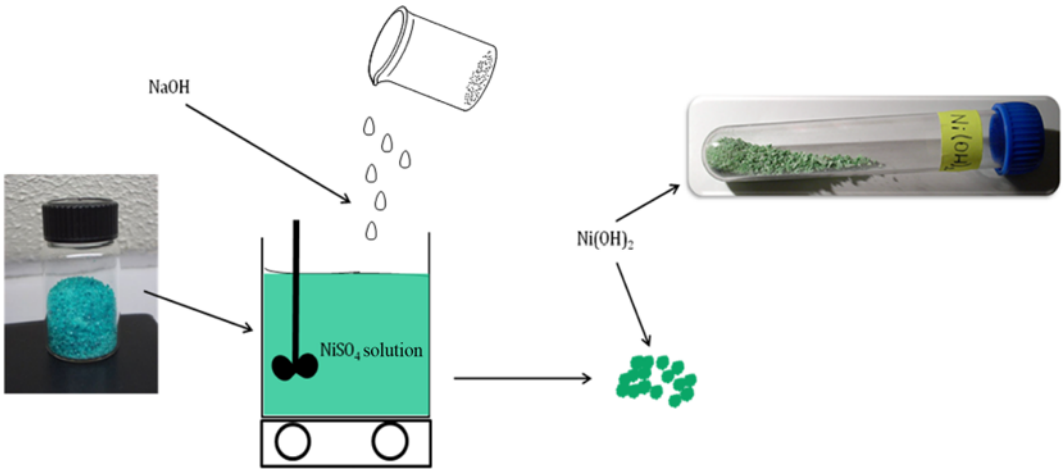

Fig. 3. Schematic of direct precipitation methods.

cess was continued until solution pH arrived at 11 (Eq. (6)).

$$NiSO_4 + 2NaOH \rightarrow Ni(OH)_2 + Na_2SO_4 \quad (6)$$

All products were collected, washed several times with deionized water, and dried in an oven at 110 °C for 24 h. NiO nanoparticles were derived from the precursor of $Ni(OH)_2$ by thermal decomposition at 350 °C for 1 h at air atmosphere.

3. Characterization

The phase composition and structure of nanoparticles were characterized by X-ray diffraction (XRD) on a Bruker-binary v3 diffractometer (Cu K_α, λ=0.15418 nm). Detection and characterization of all products in every method and during all procedures could be distinct by the use of XRD pick sharpness. The morphology and size of nanoparticles were characterized using FESEM (HITACHI S-4160, JAPAN). The FT-IR spectra of samples were recorded in the range of 400 to 4,000 cm^{-1} (Unicam 2400 spectrometer).

RESULTS AND DISCUSSION

A typical XRD pattern of the as-prepared products is shown in Fig. 4. Strong and sharp diffraction peaks suggest the precursor powders, produced by chemical homogeneous precipitation procedure in various decomposing $[Ni(NH_3)_6]^{2+}$ complex methods are well crystallized. The sharp diffraction peaks in the patterns (001), (100), (101), (102), (110), (111), (200), (201) and (201) can be exactly indexed to β-$Ni(OH)_2$ with a hexagonal structure. XRD pattern of method (a) precipitates as shown in Fig. 4(a) have more significantly sharp peaks than decomposing methods (b) and (c). This indicates that the precipitates were crystalline. The mechanism for synthesis of precursor in methods (b) and (c) is releasing Ni^{2+} ions (Eq. (3) and (4)). Based on the above-mentioned equations (Eqs. (3) and (4)), production of both $Ni(OH)_2$ and $Ni(OH)_x(SO_4)_y$ was predicted in viewpoint of scientific aspects, but based on the XRD spectra only $Ni(OH)_2$ particles have been detected. Detection of basic equation (Eq. (3)) which has the main role in the process could be considered by the use of XRD diagrams. At first, the $[Ni(NH_3)_6]^{2+}$ complex ions were very stable in the high concentration of NH_3. By decreasing concentration of NH_3, the reaction (7) has been shifted to the right side of reaction and complex ions gradually decomposed to Ni^{2+} and NH_3, so that the concentration of nickel ions increased [36].

$$[Ni(NH_3)_6]^{2+} \rightarrow Ni^{2+} + 6NH_3 \quad (7)$$

Vishnu and Subbanna synthesized $Ni(OH)_2$ nanoparticles through the complexation-precipitation method using 0.1 M $Ni(NO_3)_2$ and 0.1 KOH. The required time for reaction with these materials is up to 6 hours while in our experiment the reaction time for synthesizing $Ni(OH)_2$ is less than 2 hours, which is more efficient than Vishnu's route [37].

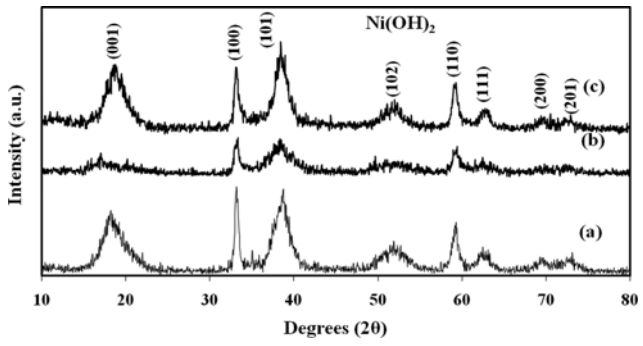

Fig. 4. X-ray diffraction of the spectrum of precursor powders that precipitated by (a) NaOH, (b) heating and (c) diluting methods.

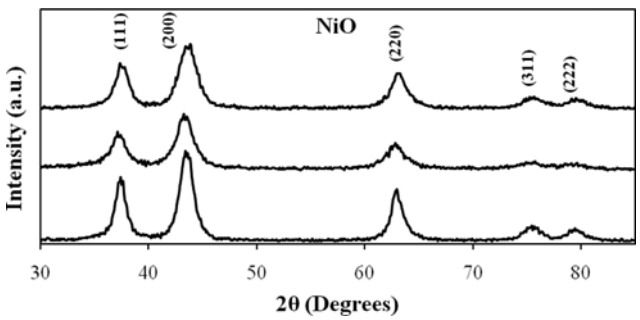

Fig. 5. X-ray diffraction of the spectrum of NiO powders that precipitated by (a) NaOH, (b) heating and (c) diluting methods.

Table 1. Mean crystallite size of $Ni(OH)_2$ and NiO obtained from different precipitation method

Precipitate agent	Mean crystallite size (nm)	
	$Ni(OH)_2$	NiO
NaOH (method a)	10	16
Heating (method b)	11	18
Diluting (method c)	8	12

As-prepared β-$Ni(OH)_2$ powders were calcinated at 350 °C for 1 h to obtain NiO nanoparticles. The X-ray diffraction pattern of NiO powders are shown in Fig. 5. All peaks (111), (200), (220), (311) and (222) coordinated to NiO phase with cubic structure. Although there is a complex agent and sodium hydroxide, no characteristics peaks of impurities such as NH_3, NaOH or other precursor compounds were observed, indicating that β-$Ni(OH)_2$ has been converted to NiO completely. X-ray diffraction pattern results showed, NiO powders obtained from method (a) have better crystallite quality than other methods. The mean crystallite sizes of precursor of three methods are shown in Table 1. The amounts for crystallite sizes were obtained from the Scherrer formula, $d=K\lambda/B\cos\theta$, where d represents the grain size; K=0.89 is the Scherrer constant related to the shape and index (hkl) of the crystals; λ is the wavelength of the X-ray (Cu Kα, λ=0.15418 nm); θ is the diffraction angle of the peak; and B stands for the full-width at half-height of the peaks (in radian) given by $B^2=Bm^2-Bs^2$, where Bm is the full-width at half maximum (FWHM) of the sample and Bs is the half-width of a standard sample with a known crystal size greater than 100 nm; the effect of instrumental broadening on the reection peaks is calibrated [38].

While, the crystallite size of diluting method is the lowest, the obtained powders do not have good crystallite quality. Among the NiO powders of three methods, the diffraction peaks in Fig. 5(a) have the strongest intensity and the sharpest shape, indicating that the sample prepared in method (a) has the best crystallization. So that, the best method for synthesis NiO nanoparticles based on crystallite quality and size, is method (a).

FESEM micrographs of the NiO nanoparticles synthesized in three precipitating methods are demonstrated in Fig. 6. This image confirms that NiO powders obtained in precipitating method (a) have uniform spherical nanoparticles with a diameter in the range of 40-60 nm. These nanoparticles are really proper for the photocatalytic usage, for example, in environmental remediation. Also, nanoparticles of NiO demonstrated better photocatalytic efficiency than some prominent previously used photocatalysts like TiO_2 for the degradation of some contaminants, especially phenol derivatives [39]. The FESEM image of the second precipitating method shows nanoflakes of NiO powders with a thickness about 30 nm Fig. 6(b). Fig. 6(c) illustrates NiO nanoparticles obtained in third precipitation method (diluting method). The morphology of the NiO nanoparticles achieved in this method is comparable to shape of NiO nanoparticles obtained in heating precipitation method with a thickness of about 40 nm. The size of synthesized NiO is less than the nanostructured particles produced from $NiSO_4$ and NaOH solutions [40].

As expected, NiO nanoparticle morphology is flake form in heating and diluting precipitation methods [41]. But, the morphology of NiO nanoparticles produced in method (a) is changed to spherical shape. It was due to increasing growth rate of the NiO nucleus. In other words, crystallization and growth of NiO powders occurred in very short time, so that the nanoparticles did not have enough time for effective accumulation and throughout growth in different directions.

To study the effect of complex agent, NiO powders were prepared by direct precipitation method, in absence of the complex agent. Fig. 7 depicts X-ray diffraction pattern of $Ni(OH)_2$ and NiO powders obtained from direct precipitation method. Based on the

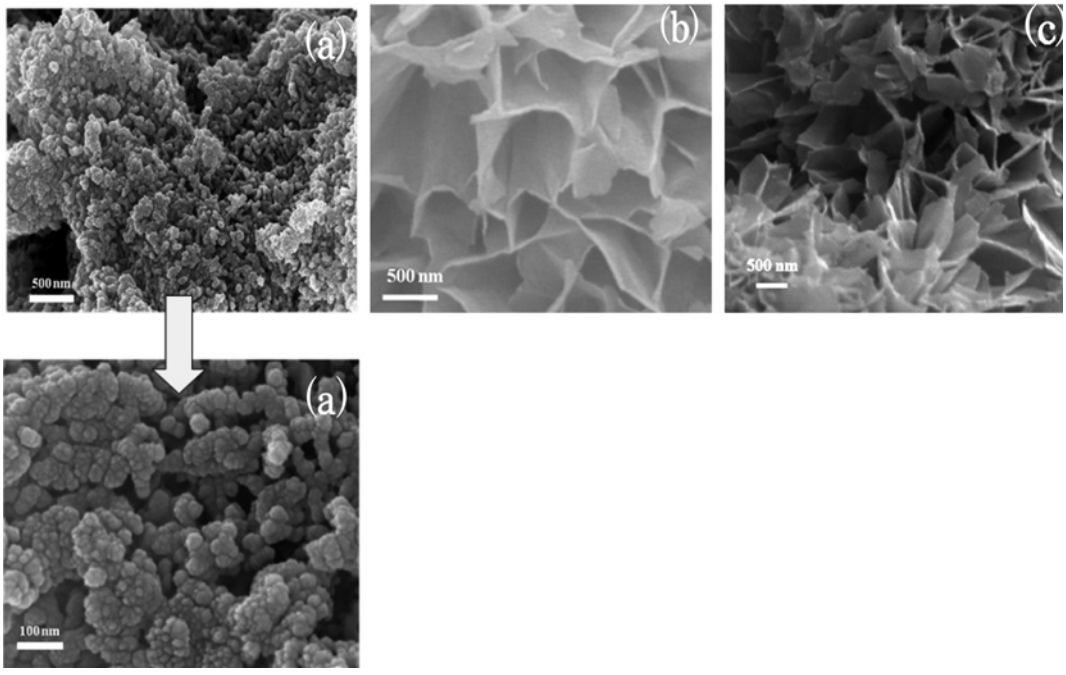

Fig. 6. FESEM micrographs of the NiO nanoparticles that precipitated by (a) NaOH, (b) heating and (c) diluting methods.

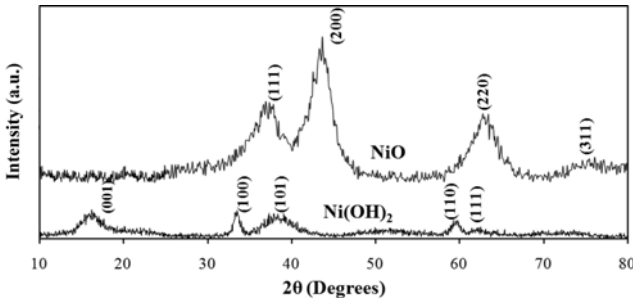

Fig. 7. X-ray diffraction of the spectrum of (a) $Ni(OH)_2$ and (b) NiO powders that produced by direct precipitation method.

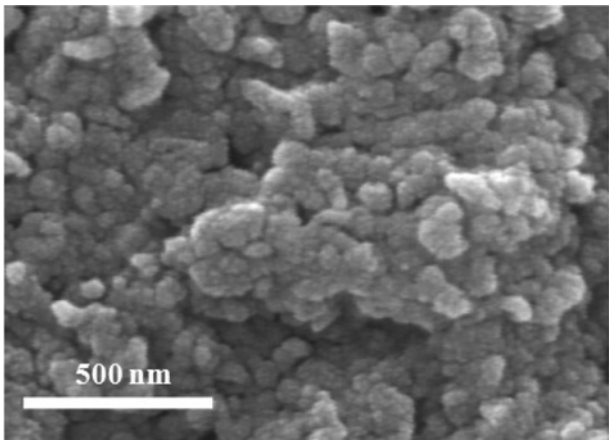

Fig. 8. FESEM micrographs of the NiO powders that produced by direct precipitation method.

XRD pattern of $Ni(OH)_2$ Fig. 7(a), the produced powders have lower crystallite quality than complex method nanoparticles. Fig. 7(a) indicates that all peaks in XRD pattern correspond to NiO phase, but it does not have good crystallite quality. It is due to the formation of colloidal particles that cannot be changed to a crystallite state. As a result, these colloidal particles caused the broadening of NiO powders peaks. The FESEM image of NiO powders clearly shows the agglomerated shapeless particles (Fig. 8). This morphology of NiO direct precipitation powders confirms the result of X-ray diffraction pattern.

In complex precipitation method, it seems that the presence of a complex agent in solution provides a controllable content of Ni^{2+} ions for precipitating of $Ni(OH)_2$. In other words, Ni ions are trapped inside of complex agent, and $Ni(OH)_2$ nucleus will be formed with low rates at a constant time. Therefore, $Ni(OH)_2$ could be grown in adequate time period and form appropriate morphology. Also, the $Ni(OH)_2$ components could be placed in proper crystalline position, which then leads to increase crystallinity of obtained powders [36,41].

FT-IR spectra were used to characterize and also confirm the synthesized NiO nanoparticles and expected bonding which were obtained in three complex precipitation and direct precipitation routes (Fig. 9(a)-(d)). As can be seen, all samples are NiO phase due to the strong peak of 430 cm^{-1} which corresponds to the vibrational Ni-O band [41]. The bands 1,030 cm^{-1} and 1,084 cm^{-1} can be attributed to the SO_4^{2-} due to presence of a minor content of sulfate substance. The SO_4^{2-} bands in complex precipitation routes are less than direct precipitation. The bands at 1,353 cm^{-1} and 1,592 cm^{-1} correspond to presence of CO_3^{2-} anion. The CO_3^{2-} anion is formed by dissolving CO_2 gas in the solution during the reaction. Broad peak at 3,415 cm^{-1} is related to O-H stretching vibration band, which could be due to the absorbed water in structure of NiO powders. Undoubtedly, using a middle step of complex production reaction amount of SO_4^{2-}, CO_3^{2-} and ^-OH anions could be a decrease in NiO nanopowders.

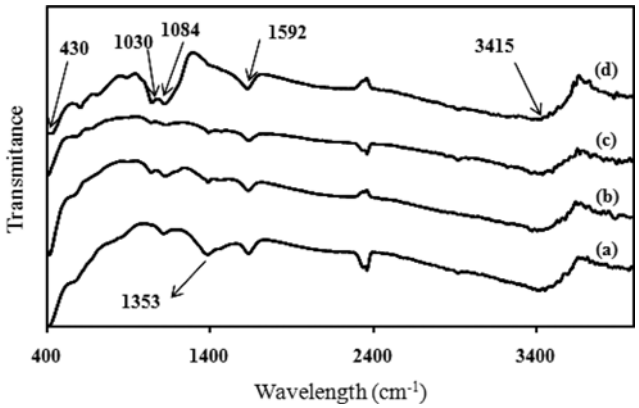

Fig. 9. FT-IR spectra of NiO nanoparticles that obtained (a) NaOH, (b) Heating, (c) Diluting complex-precipitation, (d) Direct precipitation methods.

CONCLUSIONS

NiO nanoparticles have been successfully fabricated by chemical homogeneous precipitation (CHP) using ammonia and $NiSO_4 \cdot 6H_2O$ as complex agent and raw material, respectively. Different morphology of NiO nanoparticles can be produced by changing Ni^{2+} complex decomposition method. The results indicated that the best condition for synthesizing spherical NiO shape was using NaOH as decomposed agent. Consequently, the effect of complex agent on the crystallization and growth of NiO powders was studied. Utilizing ammonia as complex agent, crystalline state and particles size distribution of NiO nanoparticles improved. FT-IR spectrum results confirmed that the NiO nanoparticles which were synthesized by CHP method had minimum amount of anions and impurities.

REFERENCES

1. J. Moghaddam, S. Kolahgar-Azari and S. Karimi, *Ind. Eng. Chem. Res.*, **51**, 3224 (2012).
2. Y. He, K. Vinodgopal, M. Ashokkumar and F. Grieser, *Res. Chem. Intermed.*, **32**, 709 (2006).
3. R. M. Kassab, K. T. Jackson, O. M. El-Kadri and H. M. El-Kaderi, *Res. Chem. Intermed.*, **37**, 747 (2011).
4. D. Adler and J. J. Feinleib, *Phys. Rev. B: Condens. Matter*, **2**, 3112 (1970).
5. I. Hotovy, J. Huran, L. Spiess, S. Hascik and V. Tehacek, *Sens. Actuators, B*, **57**, 147 (1999).
6. E. L. Miller and R. E. Rocheleau, *J. Electrochem. Soc.*, **144**, 3072 (1997).

7. Y. P. Wang, J. W. Zhu, X. J. Yang, L. D. Lu and X. Wang, *Thermochim. Acta*, **437**, 106 (2005).
8. R. C. Makkus, K. Hemmes and J. H. W. D. Wir, *J. Electrochem. Soc.*, **141**, 3429 (1994).
9. M. Ghosh, K. Biswas, A. Sundaresan and C. N. R. Rao, *J. Mater. Chem.*, **16**, 106 (2006).
10. X. Wang, L. J. Ye, P. Hu and F. L. Yuan, *Cryst. Growth Des.*, **7**, 2415 (2007).
11. C. N. Huang, S. Y. Chen and P. Shen, *J. Phys. Chem. C*, **111**, 3322 (2007).
12. B. Zhao, X. K. Ke and J. H. Bao, *J. Phys. Chem. C*, **113**, 14440 (2009).
13. M. S.Wu and H. H. Hsieh, *Electrochim. Acta*, **53**, 3427 (2008).
14. J. R. A. Sietsma, J. D. Meeldijk, J. P. D. Breejen, M. V. Helder, A. J. V. Dillen, P. E. D. Jongh and K. P. D. Jong, *Angew. Chem. Int. Ed.*, **46**, 4547 (2007).
15. L. X. Yang, Y. J. Zhu, H. Tong, Z. H. Liang, L. Li and L. J. Zhang, *J. Solid State Chem.*, **180**, 2095 (2007).
16. C. K. Xu, K. Q. Hong, S. Liu, G. H. Wang and X. N. Zhao, *J. Cryst. Growth*, **255**, 308 (2003).
17. L. L. Wu, Y. S. Wu, H. Y. Wei, Y. C. Shi and C. X. Hu, *Mater. Lett.*, **58**, 2700 (2004).
18. M. B. Zheng, J. M. Cao, Y. P. Chen, X. J. Ma, S. G. Deng and J. Tao, *Chem. Lett.*, **34**, 1174 (2005).
19. W. Xing, F. Li, Z. F. Yan, H. M. Cheng and G. Q. Lu, *Int. J. Nanosci.*, **3**, 321 (2004).
20. X. M. Liu, X. G. Zhang and S. Y. Fu, *Mater. Res. Bull.*, **41**, 620 (2006).
21. L. Y. Bai, F. L. Yuan, P. Hu, S. K. Yan, X. Wang and S. H. Li, *Mater. Lett.*, **61**, 1698 (2007).
22. X. M. Ni, Y. F. Zhang, D. Y. Tian, H. G. Zheng and X. W. Wang, *J. Cryst. Growth*, **306**, 418 (2007).
23. A. Al-Hajry, A. Umar, M. Vaseem and M. S. Al-Assiri, *Superlattices Microstruct.*, **44**, 216 (2008).
24. L. P. Zhu, G. H. Liao, Y. Yang, H. M. Zhao and J. G. Wang, *Nanoscale Res. Lett.*, **4**, 550 (2009).
25. H. Z. Wang and Y. T. Qian, *Cryst. Res. Technol.*, **45**, 545 (2010).
26. V. Rehacek, P. Siciliano, S. Capone and L. Spiess, *Thin. Solid. Films*, **418**, 9 (2002).
27. T. Y. Kim, J. Y. Kim, S. H. Lee, H. W. Shim, S. H. Lee, E. K. Su and K. S. Nahm, *Synthetic Met.*, **144**, 61 (2004).
28. F. Li, H. Chen, Ch. Wang and K. Hu, *J. Electroanal. Chem.*, **531**, 53 (2002).
29. S. A. Needham, G. X. Wang and H. K. Liu, *J. Power. Sources*, **159**, 254 (2006).
30. M. Gondal, M. Sayeed and Z. Seddigi, *J. Hazard. Mater.*, **155**, 83 (2008).
31. D. B. Kuang, B. X. Lei, Y. P. Pan, X. Y. Yu and Ch. Y. Su, *J. Phys. Chem. C*, **113**, 5508 (2009).
32. Q. Yang, J. Sha, X. Maa and D. Yang, *Mater. Lett.*, **59**, 1967 (2005).
33. M. Salavati-Niasari, N. Mir and F. Davar, *J. Alloy. Compd.*, **493**, 163 (2010).
34. V. V. Plashnitsa, V. Gupta and N. Miura, *Electrochim. Acta*, **65**, 6941 (2010).
35. X. Y. Deng and Z. Chen, *Mater. Lett.*, **58**, 276 (2004).
36. P. V. Kamath and G. N. Subbanna, *J. Appl. Electrochem.*, **22**, 478 (1992).
37. Z. Wei, H. Qiao, H. Yang, C. Zhang and X. Yan, *J. Alloy. Compd.*, **479**, 855 (2009).
38. B. D. Cullity, *Elements of X-ray diffraction*, First Ed., Addison Wesley, Massachusetts (1956).
39. A. D. Paola, E. García-López, G. Marcì and L. Palmisano, *J. Hazard. Mater.*, **211-212**, 3 (2012).
40. Q. S. Song, Y. Y. Li and S. L. I. Chan, *J. Appl. Electrochem.*, **35**, 157 (2005).
41. C. Xu, K. Hong, Sh. Liu, G. Wang and X. Zhao, *J. Cryst. Growth*, **255**, 308 (2003).